

We are IntechOpen, the world's leading publisher of Open Access books Built by scientists, for scientists

5,900

Open access books available

145,000

International authors and editors

180M

Downloads

Our authors are among the

154

Countries delivered to

TOP 1%

most cited scientists

12.2%

Contributors from top 500 universities



WEB OF SCIENCE™

Selection of our books indexed in the Book Citation Index
in Web of Science™ Core Collection (BKCI)

Interested in publishing with us?
Contact book.department@intechopen.com

Numbers displayed above are based on latest data collected.
For more information visit www.intechopen.com



Broadside Pattern Correction Techniques for Conformal Antenna Arrays

Irfan Ullah, Shahid Khattak and Benjamin D. Braaten

Abstract

Phase compensation techniques based on projection method and convex optimization (phase correction only) for comparing the maximum gain of a phase-compensated conformal antenna array have been discussed. In particular, these techniques are validated with conformal phased array antenna attached to a cylindrical-shaped surface with various radii of curvatures. These phase compensation techniques are used to correct the broadside radiation pattern. It is shown that the maximum broadside gain compensated is still less than the gain of a linear flat array for any surface deformation. This fundamental maximum compensated gain limitations of the phase compensation techniques can be used by a designer to predict the maximum broadside obtainable theoretical gain on a conformal antenna array for a particular deformed surface.

Keywords: conformal antennas, phased arrays, antenna radiation patterns, convex optimization, microstrip arrays

1. Introduction

Conformal antenna arrays are beneficial for applications that need an antenna to be placed on a non-flat surface, for example, on the fuselage of a UAV/airplane in the aerospace industry [1–3], implantable sensors in wearable networks [4–8], and satellite communications [9–11]. One of the main advantages of using conformal antenna is its structural integration ability on singly curved (e.g., a wedge/cylinder) [12–15] and doubly curved (like a sphere) surfaces [16]. This can be very useful in applications where using definite flat surface may not be a practical design choice. Another exciting application of conformal antenna array is at the base station in a cellular mobile communication system. Today, mobile service providers are utilizing three separate antenna panels (dipole or monopole array) in a cell for a 120° sector coverage. What about, if one cylindrical array is used instead of three dipole arrays [17]? This can result in a much smaller transmitter requirement with 360° azimuthal coverage plus reduced base station size at a lower cost (specifically beneficial in crowded residential areas where cellular companies have to rent the space for base station installation).

On the other hand, these curved surfaces may be subjected to intentional (e.g., flexing wings of a UAV/aircraft) and/or unintentional (bending of aircraft wings due to severe weather conditions/vibrations) forces that change the shape of the

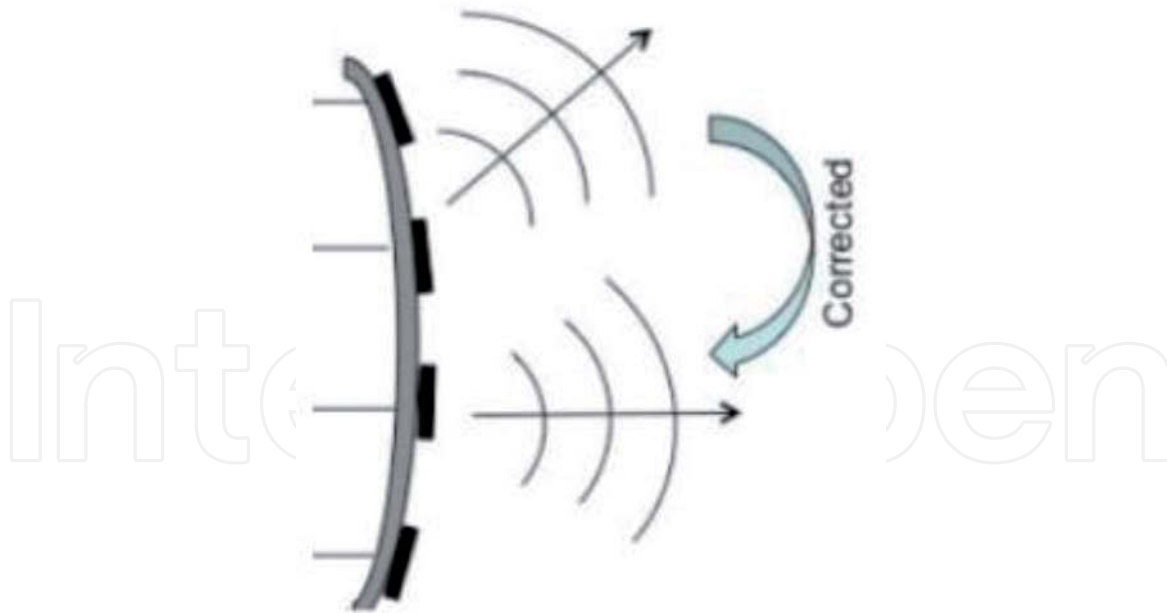


Figure 1.
Array on a conformal surface.

surface [12]. As a result, the radiation pattern of the conformal antenna array is changed as shown in **Figure 1**. The results in [18] indicate that directivity of conformal antenna array can be reduced by 5–15 dB. In the literature, various methods have been proposed to compensate the reduction in directivity and to improve/correct the radiation pattern of a conformal antenna array. In [1–3, 11, 19–21], mechanical calibration techniques have been used to steer the main beam on a conformal surface in the desired direction. In [12, 13, 15, 16, 22–25], projection method of [26] is used to correct the main beam direction of a deformed/flex surface. In [27–30], various optimization algorithms have been used to control the radiation pattern of conformal antenna arrays. In summary, it has been shown that the radiation pattern of a conformal antenna array can be improved with different calibration techniques, signal processing algorithms, sensor circuitry, and phase and amplitude adjustments.

This chapter will focus on phase compensation of four-element conformal cylindrical antenna array using (1) projection method and (2) convex optimization method. First, a brief introduction and working principle of phase compensation is presented using projection method. Then, array factor expression will be derived to compensate the radiation pattern of conformal cylindrical array. Then, the convex optimization algorithm will be discussed to compute the array weights for pattern recovery of conformal cylindrical array. Then, compensated gain using both the methods will be compared to linear flat array to explore the gain limitations of these compensated techniques for conformal antenna arrays. Finally, conclusion and future work are presented.

2. Projection method for pattern recovery of conformal antenna array

The projection method in [26] and its further exploration in [12, 15, 22] are adopted here to describe the behavior of the conformal antenna array shown in **Figure 2**. For discussion, consider the problem where the flat antenna array is placed on the singly curved surface shaped as a cylinder with radius r as shown in **Figure 2**. The position of each antenna element on the cylinder is represented

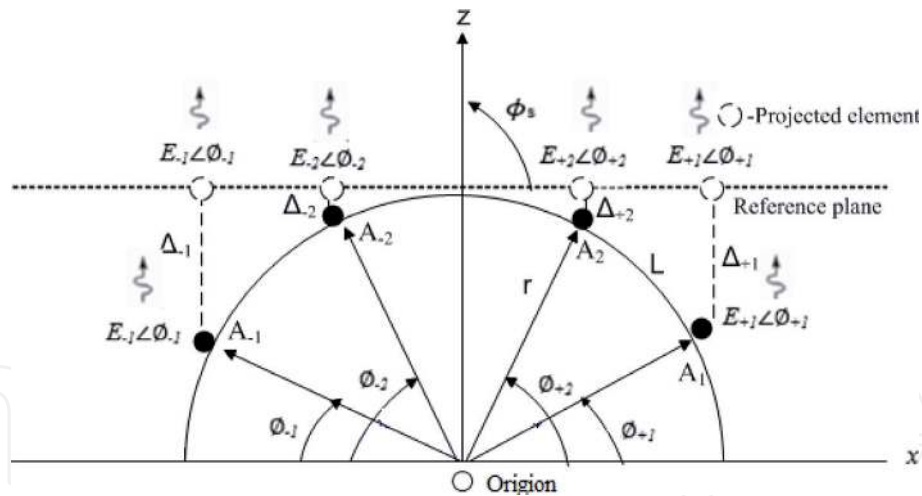


Figure 2.
 Phase compensation of a conformal cylindrical antenna array.

as $A_{\pm n}$, $n = 1, 2$ (for four antenna elements on the cylindrical surface). If each antenna element on the cylindrical surface is excited with uniform amplitudes and phases, that is, if excitation weights $w_n = 1e^{j\theta}$ put on all elements, then the E-fields radiated from the antenna elements will arrive at the reference plane with different phases. This phase difference is due to the different path lengths experienced by the radiated E-fields in the z direction while reaching to the reference plane. Because phases of E-fields radiated from $A_{\pm 1}$ are not the same as those radiated by $A_{\pm 2}$, the radiation may not necessarily be constructively added broadside to the array (i.e., with $\phi_s = 90^\circ$). If the E-fields $E_{\pm n}e^{j\phi_{\pm n}}$ from antenna elements are ensured to arrive at the reference plane with the same phase, then constructive interference will result in a broadside radiation pattern and therefore pattern recovery toward the broadside is possible. The delayed phase of E-fields due to free-space propagation ($-k\Delta_{\pm n}$) from antenna elements on the conformal surface to the reference plane can be compensated (corrected) by exciting the elements with phase advance ($+k\Delta_{\pm n}$). This will cause the E-fields from antenna elements to arrive at the reference plane with same phase and will cause constructive broadside radiation pattern in the +z direction.

To compute this compensated phase, the antenna elements are projected on the reference plane and then the distances from antenna elements on cylindrical surface (shown as black dots) to the projected elements on the reference plane (shown as dashed circles) are calculated. Suppose Δ_{-1} , Δ_{-2} , Δ_2 , and Δ_1 denote the distances from the elements A_{-1} , A_{-2} , A_2 , and A_1 , respectively, to the reference plane (or the projected elements on the reference plane).

2.1 Computing the distance to the projected elements

The distance from the antenna elements on the cylinder to the projected elements on the reference plane can be computed using:

$$\Delta_{\pm n} = r - r \sin \phi_{\pm n} \quad (1)$$

where r is the radius of the cylinder and $\phi_{\pm n}$ is the angular position of antenna elements on the cylinder. Using the relation of $\mathbf{L} = r\boldsymbol{\theta}$, the angular positions of antenna elements can be calculated, where $L = \lambda/2$ is the inter-element distance on the cylindrical surface.

2.2 Computing the compensated phase

The required compensated phase to correct the broadside radiation pattern of a conformal cylindrical antenna array in **Figure 2** is then given by:

$$\delta_{\pm n}^c = +k \Delta_{\pm n} \quad (2)$$

where k is the free-space wave number.

2.3 Array factor expression

To analytically compute the corrected (compensated) radiation pattern and validate with simulation results, the following compensated array factor AF_c is used [18, 31]:

$$AF_c = AF e^{j\delta_{\pm n}^c}, \quad (3)$$

where $\delta_{\pm n}^c$ can be computed using Eq. (2) and the array factor (AF) expression for antennas on conformal surfaces is [18]:

$$AF = \sum_{n=1}^N F_n(\theta, \phi) w_n e^{jk[x_n \sin\theta + z_n \cos\theta]}, \quad (4)$$

where k is the free space wave number, N is number of antenna elements, (x_n, z_n) is the location of n th antenna element on the conformal surface, and $F_n(\theta, \phi)$ is the individual element pattern in **Figure 2**. $w_n = I_n e^{j\Delta\phi}$ is the complex weighting function required to drive the n th antenna element.

For this work, the phase difference $\Delta\phi$ between adjacent antenna elements was made zero, and the amplitude tapering coefficient I_n was kept equal to 1 (uniform excitation). Using Eqs. (1)–(4), the expression for corrected array factor is given by:

$$AF_c = F_1(\theta, \phi) e^{jk\Delta_{-1}} e^{jk[x_1 \sin\theta + z_1 \cos\theta]} + F_2(\theta, \phi) e^{jk\Delta_{-2}} e^{jk[x_2 \sin\theta + z_2 \cos\theta]} \\ + F_3(\theta, \phi) e^{jk\Delta_{+2}} e^{jk[x_3 \sin\theta + z_3 \cos\theta]} + F_4(\theta, \phi) e^{jk\Delta_{+1}} e^{jk[x_4 \sin\theta + z_4 \cos\theta]} \quad (5)$$

$F_1(\theta, \phi) = \cos(\theta + \phi_{-1})$ and $F_2(\theta, \phi) = \cos(\theta + \phi_{-2})$ are the element patterns for the two left antenna elements and $F_3(\theta, \phi) = \cos(\theta - \phi_{+1})$ and $F_4(\theta, \phi) = \cos(\theta - \phi_{+2})$ are the element patterns for the two right antenna elements on the cylindrical surface in **Figure 2**. It should be noted that for linear array, the element pattern is $\cos(\theta)$ as all the elements are pointing towards zenith (that is towards $\phi_i = 0^\circ$). However on conformal surfaces, the individual element patterns become geometry dependent. For example, as can be seen in **Figure 2**, the look directions of antenna elements A_{-1} and A_{-2} are towards the angular directions ϕ_{-1} and ϕ_{-2} respectively, while the look directions of antenna elements A_1 and A_2 are towards the angular directions ϕ_1 and ϕ_2 respectively. Therefore, the element patterns are $\cos(\theta + \phi_{-1})$, $\cos(\theta + \phi_{-2})$, $\cos(\theta - \phi_1)$, and $\cos(\theta - \phi_2)$ respectively.

3. Convex optimization for pattern recovery of conformal antenna array

The broadside gain maximization problem of a conformal antenna array in **Figure 2** can be formulated as a linear constrained quadratic programming problem [32], i.e.,

$$\text{Minimize } \|\mathbf{w}_n\|,$$

Subject to

$$AF_{target} = 1, \quad (6)$$

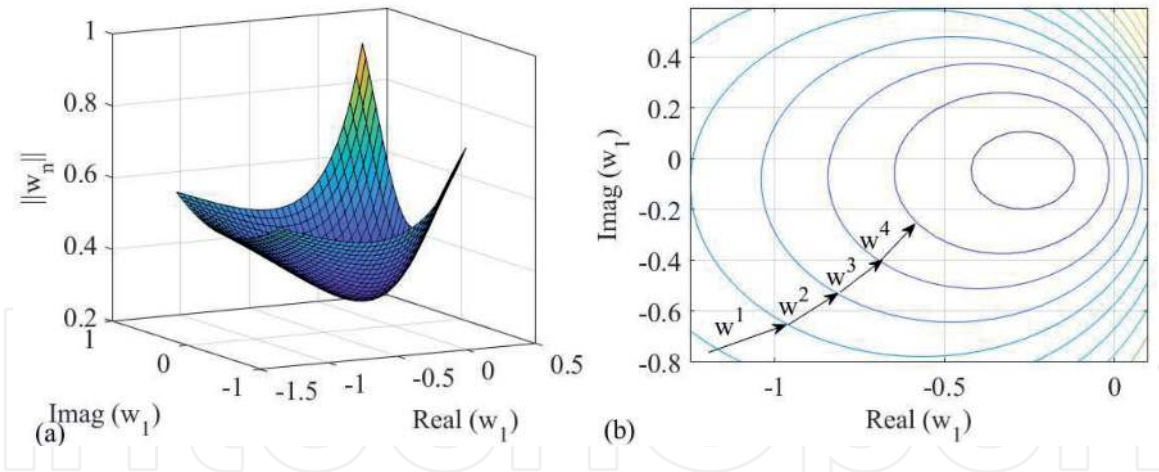


Figure 3. (a) 3D plot of the objective function plotted as a function of real (w_1) and imaginary (w_1). (b) the contour plot of the objective function with illustration of gradient descent method.

where $\mathbf{w}_n \in \mathbb{C}^{[N \times 1]}$ is the complex weighing vector, which gives the objective function $2N$ degrees of freedom. In **Figure 3(a)** the objective function plotted for the two component dimensions of the first antenna weight w_1 clearly indicates its convex form in the vicinity of the origin. The contour plots in the considered two dimensions are also presented in **Figure 3(b)**. The aspect of the contour lines along these two dimensions suggests low condition number. This well condition behavior also exists among the other degrees of freedom and results in a reduced convergence time to find the minimum within the search space.

Iterative optimization algorithms are normally adopted to find this minimum. Although second-order Newton method is able to find the solution in fewer steps, it requires evaluation of complex quadratic norm defined as the Hessian matrix $\nabla^2 \|\mathbf{w}_n\|$, which is quite complex. Since the problem is well-conditioned, even the low complexity first-order Gradient decent method can find the solution quickly. If the iteration number is represented as superscript k , then the weights update in the k^{th} iteration for Gradient descent method is given as

$$w^{(k+1)} = w^{(k)} + t^{(k)} \Delta w^k, \quad (7)$$

where $t^{(k)}$ is the scalar step size obtained through backtracking method which reduces as one gets closer to the global minimum. Δw^k is the step direction, which is chosen to maximize the negative gradient $\nabla \|\mathbf{w}_n^{(k)}\|$ at each step. The method descends in each step such that $\|\mathbf{w}_n^{(k+1)}\| \leq \|\mathbf{w}_n^{(k)}\|$, until the optimum minimum is reached, and the slope becomes positive. Since the objective function is trying to minimize the norm, the number of steps required for convergence is reduced if the starting point is chosen close to the origin. It should be noted that in this work, the algorithm was used to calculate the required compensated phases only (with uniform amplitudes). Computing the weights for phase correction using Eq. (7) to maximize the broadside gain of conformal antenna array in **Figure 2** are used in Eq. (5) to plot the corrected radiation pattern.

4. Analytical and simulation results

To analytically compute the corrected (compensated) radiation pattern and validate with simulation results, the compensated array factor AF_c in Eq. (5) was used for different radii of curvatures of the cylindrical surface in **Figure 2**.

The compensated (corrected) weights were computed using projection method in Section 2 and convex optimization in Section 3. The analytical results using Eq. (5) and CST simulation results using **Figure 2** are discussed next.

4.1 Cylindrical surface with radius of curvature $r = 8$ cm

The four-element microstrip patch antenna array on a cylindrical surface with radius $r = 8$ cm in **Figure 2** was simulated in CST simulator. The inter-element spacing was $L = \lambda/2$ at $f = 2.45$ GHz. The compensated phases for broadside pattern recovery were computed using Eq. (2) for projection method, and are tabulated in **Table 1**. For uncorrected pattern, the complex weights $w_n = 1 \angle 0^\circ$ were applied on all antenna elements in CST simulator. Next, the weights (phase correction only) for broadside pattern recovery were calculated using the optimization algorithm in Section 3 and are also tabulated in **Table 1**. The analytical and CST simulation results for $r = 8$ cm are shown in **Figure 4**. Next, the difference in gain (G_{ref}) between flat array and compensated gain of conformal array were calculated and are also given in **Table 1**. It can be seen from **Figure 4** and **Table 1** that the broadside compensated gain G_c of conformal antenna array is greater than the uncorrected gain and is less than the gain of flat array using both projection and convex optimization (phase correction only) methods. This is the fundamental limitation of both the compensation methods for broadside pattern recovery of conformal antenna arrays and should be kept in mind while designing conformal antenna array. It should be noted that convex optimization has more degrees of freedom than projection method in the sense that convex optimization gives complex weights (amplitude tapering plus phase correction), while projection method gives only phase correction (one degree of freedom). However, for broadside pattern recovery, convex optimization gives uniform amplitudes (equal to 1) and compensated phases and thus its performance is equal to projection method for broadside pattern recovery.

r (cm)	Parameter	Projection method	Convex optimization
8	δ^c (deg)	[121.67,0,0,121.67]	[-89.49,146.95,146.95,-89.49]
	G_c (dB)	6.17	6.17
	G_{ref} (dB)	0.8	0.8
10	δ^c (deg)	[101.84,0,0,101.84]	[-170.44,85.95,85.95,-170.44]
	G_c (dB)	4	
	G_{ref} (dB)	0.53	
12	δ^c (deg)	[86.95,0,0,86.95]	[114.61,26.05,26.05,114.61]
	G_c (dB)	2.74	
	G_{ref} (dB)	0.4	
15	δ^c (deg)	[70.95,0,0,70.95]	[9.66,-62.66,-62.66,9.66]
	G_c (dB)	1.765	
	G_{ref} (dB)	0.24	
30	δ^c (deg)	[36.42,0,0,36.42]	[-102.2,-139.3,-139.3,-102.2]
	G_c (dB)	0.5	
	G_{ref} (dB)	0	

Table 1. Computed parameters of conformal cylindrical array for various radii of curvatures.

4.2 Cylindrical surface with radii of curvatures $r = 10, 12, 15$ cm

When radii of curvatures of cylindrical surface array increase (less deformation), both the projection and convex optimization (phase correction only) methods recover the broadside radiation pattern with decreasing gap between corrected and uncorrected gains as shown in **Figures 5–7** and are also tabulated in **Table 1**. The gain G_c (between uncorrected and corrected) and G_{ref} (between corrected and linear) decreases with increase in r . However, it is obvious that in all cases, the

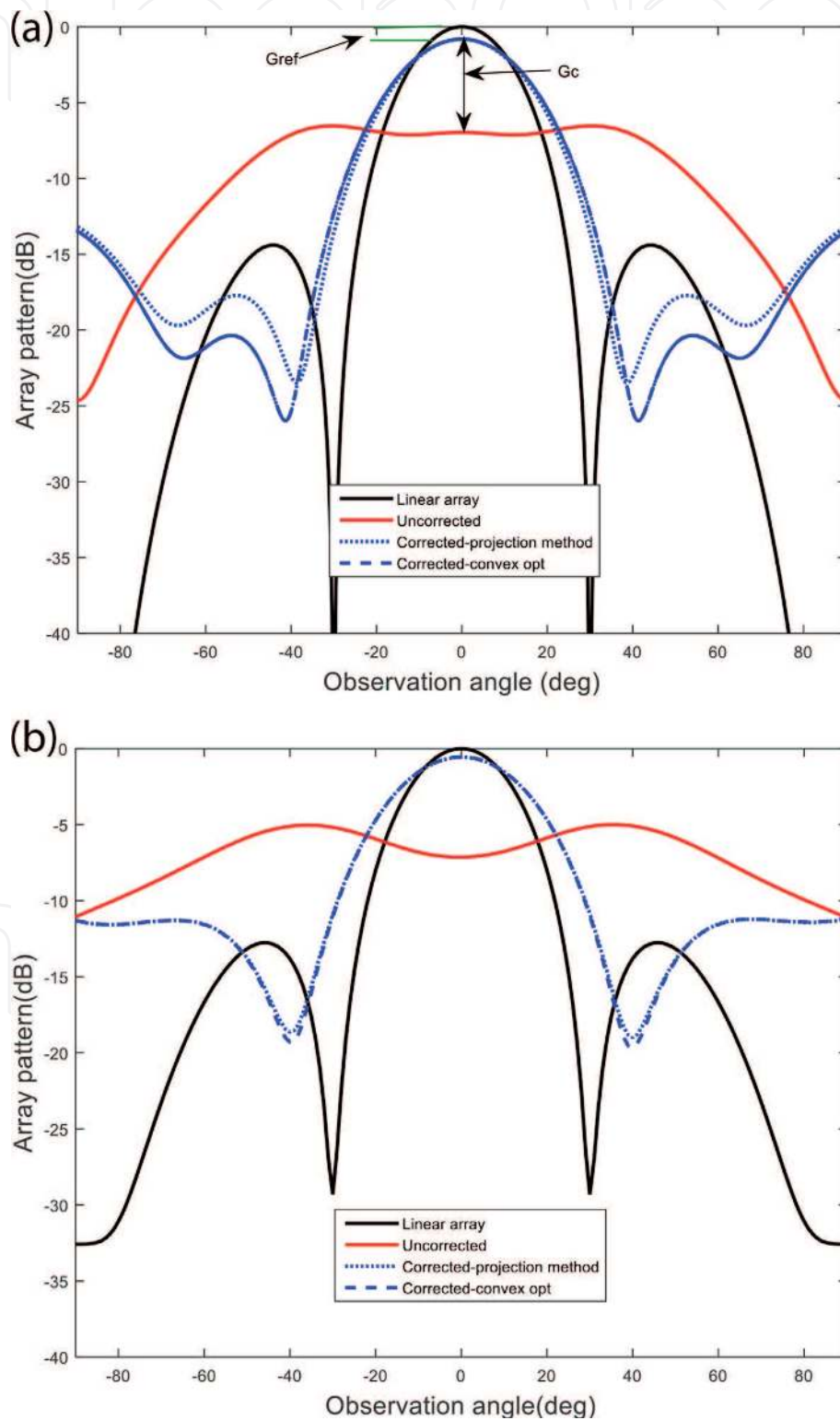


Figure 4. (a) Analytical results for phase compensation of a conformal cylindrical antenna array with $r = 8$ cm. (b) CST simulation results for phase compensation of a conformal cylindrical antenna array with $r = 8$ cm.

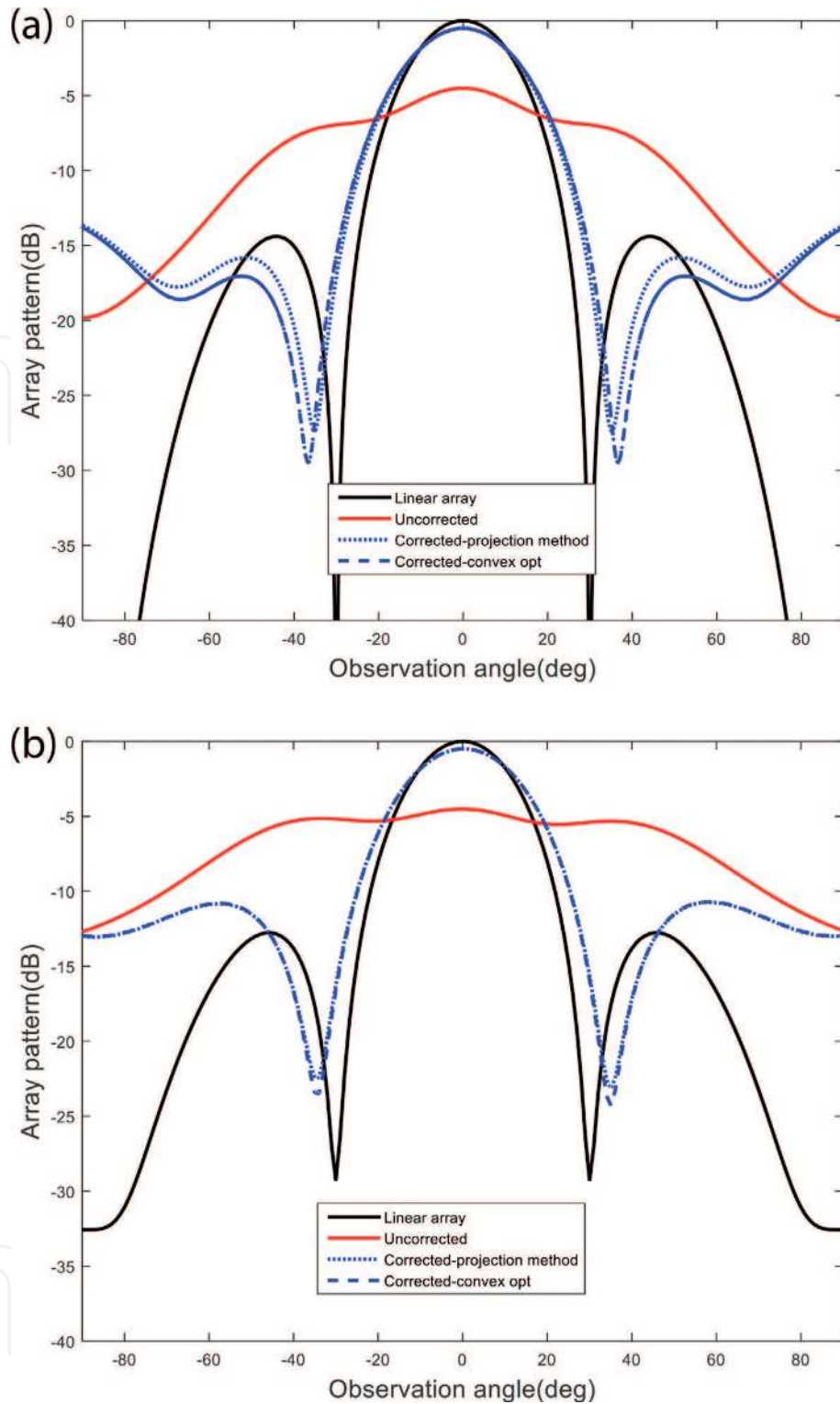


Figure 5.
 (a) Analytical results for phase compensation of a conformal cylindrical antenna array with $r = 10$ cm.
 (b) CST simulation results for phase compensation of a conformal cylindrical antenna array with $r = 10$ cm.

compensated gain is less than the ideal gain (linear array) for both projection and convex optimization methods. This is an important finding and must be kept in design stages of conformal antenna arrays.

4.3 Cylindrical surface with radii of curvatures $r = 30$ cm

In the limiting case, when the radius of curvature of conformal cylindrical array increases up to 30 cm and above (approaching flat array), the compensated gains

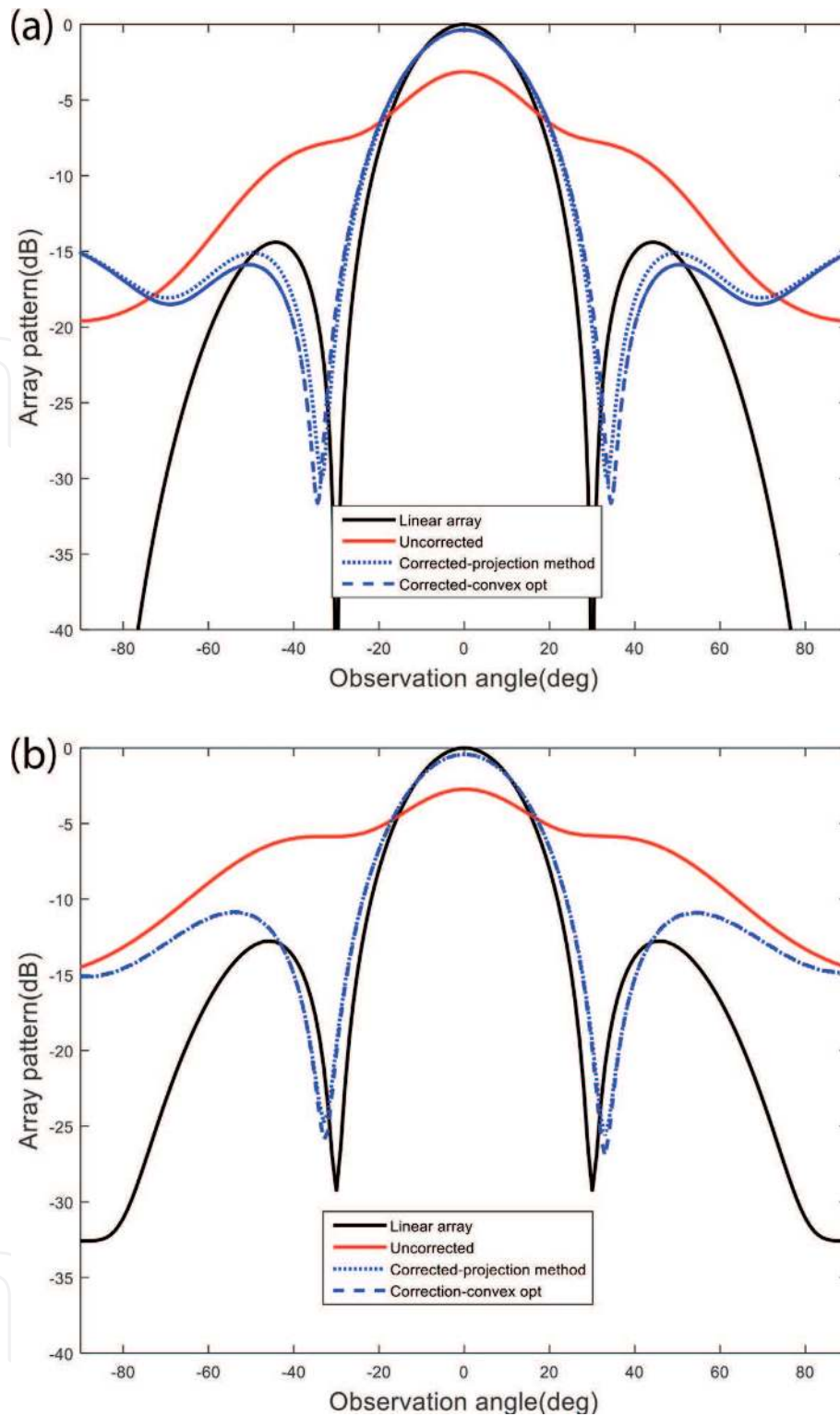


Figure 6.
(a) Analytical results for phase compensation of a conformal cylindrical antenna array with $r = 12$ cm.
(b) CST simulation results for phase compensation of a conformal cylindrical antenna array with $r = 12$ cm.

achieved from both projection and convex optimization methods nearly reaches the linear flat array gain, which is demonstrated in **Figure 8** and is shown in **Table 1**.

5. Conclusion

In this chapter, phase compensation techniques based on projection method and convex optimization (phase correction only) have been discussed for recovery

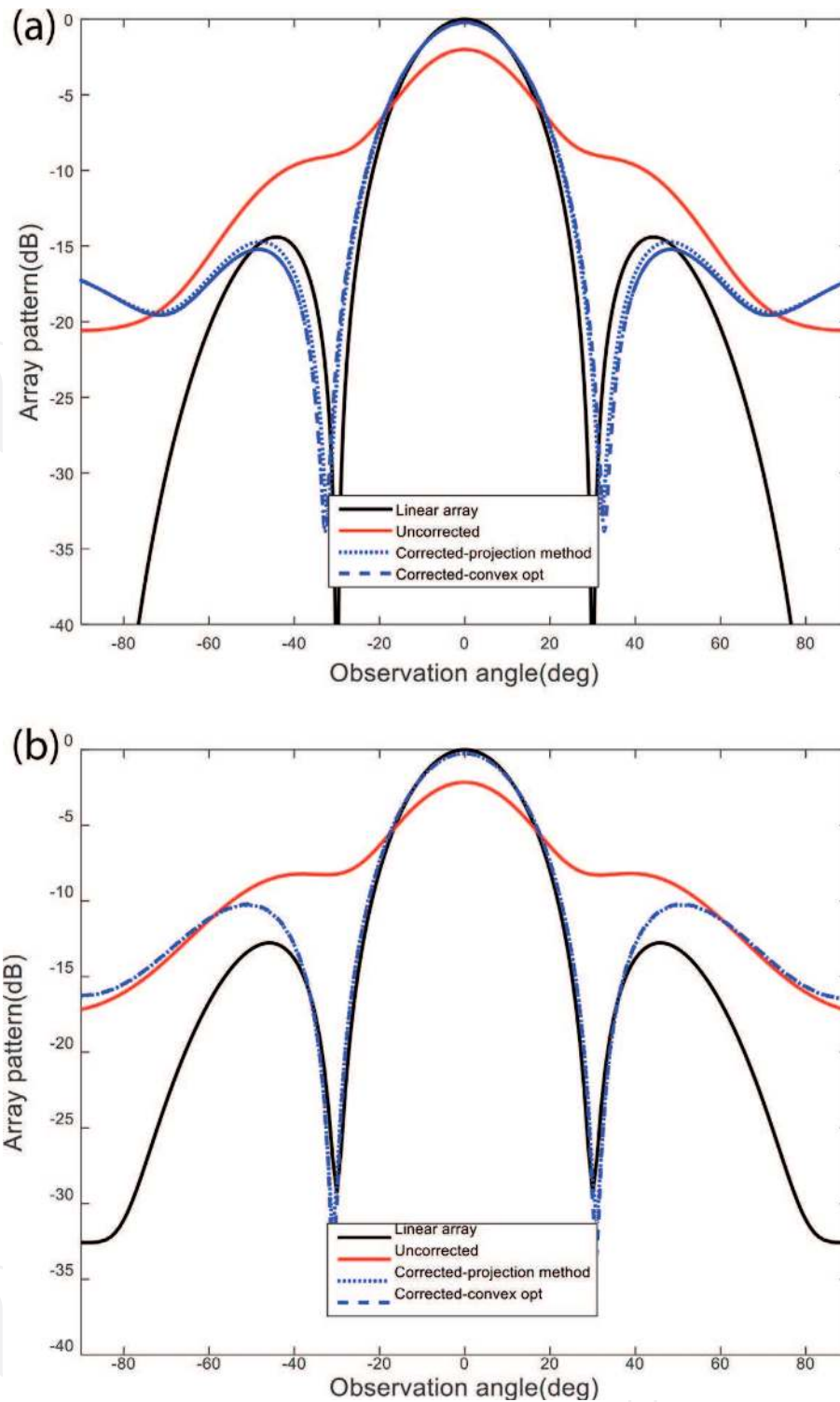


Figure 7.
 (a) Analytical results for phase compensation of a conformal cylindrical antenna array with $r = 15$ cm.
 (b) CST simulation results for phase compensation of a conformal cylindrical antenna array with $r = 15$ cm.

of broadside radiation pattern on a conformal cylindrical-shaped antenna array. The compensated gains of both the methods have been compared with linear flat antenna array. It is shown that the maximum broadside gain recovered with both the methods is less than the linear antenna array for severe deformation cases and approaches the gain of linear antenna array for less conformal deformation surfaces. The analytical expressions and convex optimization algorithm used can be used by a designer to predict the maximum possible compensated gain of conformal antenna array.

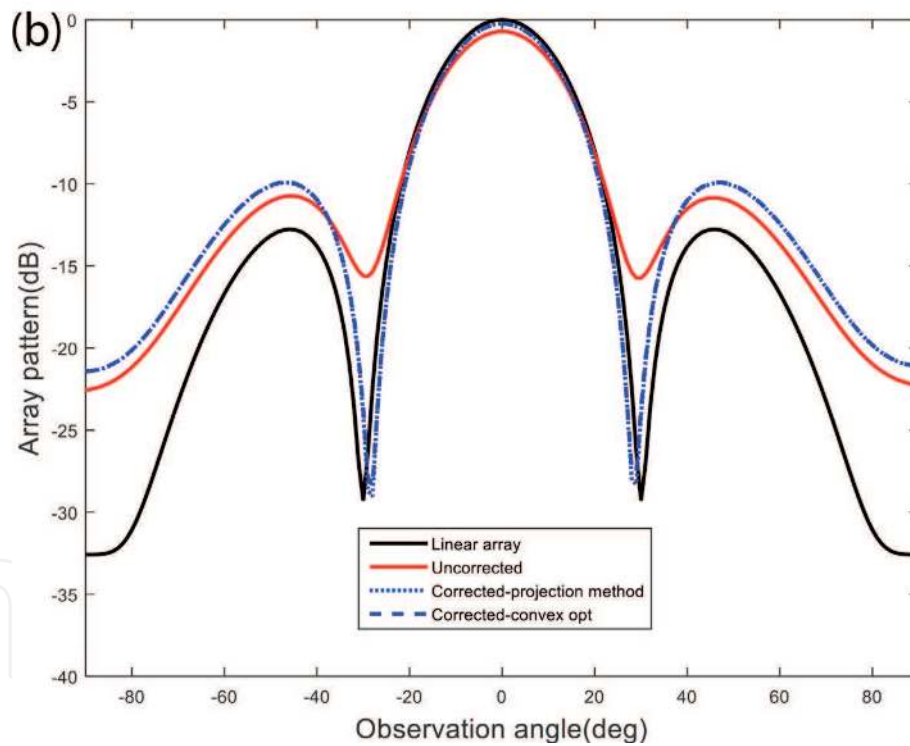
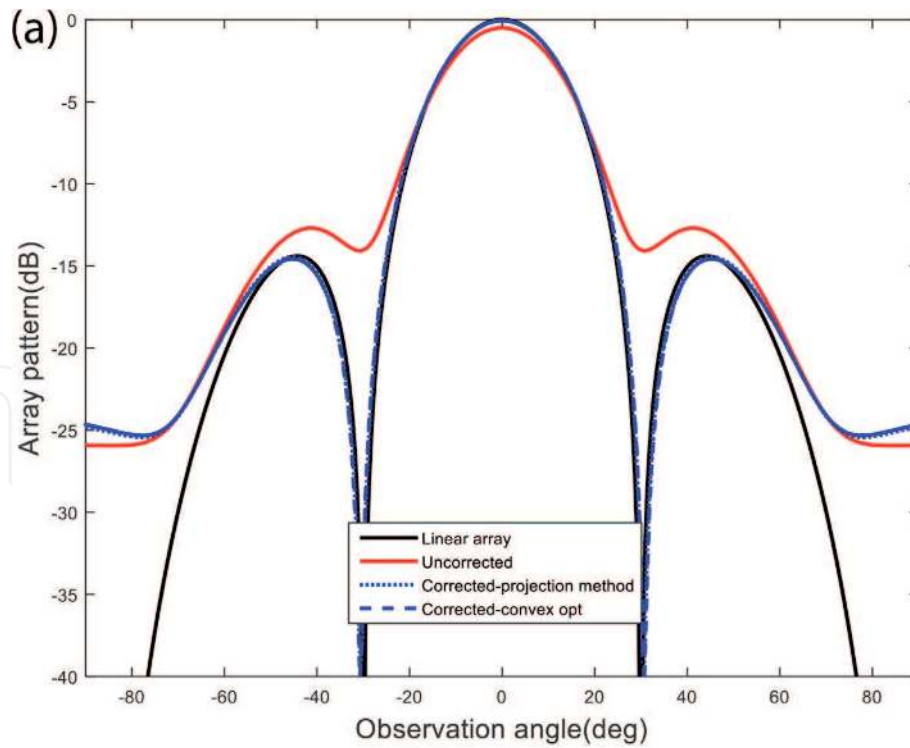


Figure 8.
(a) Analytical results for phase compensation of a conformal cylindrical antenna array with $r = 30$ cm.
(b) CST simulation results for phase compensation of a conformal cylindrical antenna array with $r = 30$ cm.

6. Future work

The proposed techniques can be extended for broadside pattern correction of conformal antenna arrays on other deformed surfaces (spherical nose of plane, flexing wings of UAV, etc.). Another interesting research can be to extend these techniques for beamforming on conformal deformed surfaces (e.g., on base station/tower of cellular companies) to improve the signal-to-noise ratio (SNR) and its

capacity. In this work, convex optimization is used to compute the compensated phases (with uniform amplitudes constraint) for recovery of broadside radiation pattern only. In practice, the technique is robust and can be used to calculate complex weights (amplitude tapering as well as phase correction), which can be further explored for beamforming applications and side lobe level control of conformal antenna arrays.

Acknowledgements

This work is supported by Ignite (NTF), Ministry of IT & Telecom, Government of Pakistan via project no. ICTRDF/TR&D/2015/04.

Author details

Irfan Ullah^{1*}, Shahid Khattak¹ and Benjamin D. Braaten²

1 Electrical and Computer Engineering Department, COMSATS University Islamabad, Abbottabad, Pakistan

2 Electrical and Computer Engineering Department, North Dakota State University, Fargo, USA

*Address all correspondence to: eengr@cuiatd.edu.pk

IntechOpen

© 2020 The Author(s). Licensee IntechOpen. This chapter is distributed under the terms of the Creative Commons Attribution License (<http://creativecommons.org/licenses/by/3.0>), which permits unrestricted use, distribution, and reproduction in any medium, provided the original work is properly cited. 

References

- [1] Schippers H, Knott P, Deloues T, Lacomme P, Scherbarth MR. Vibrating antennas and compensation techniques Research in NATO/RTO/SET 087/RTG 50. In: IEEE Aerospace Conference; 3-10 March 2007; Big Sky, MT. pp. 1-13
- [2] Wincza K, Gruszczynski S. Influence of curvature radius on radiation patterns in multibeam conformal antennas. In: Proceedings of the 36th European Microwave Conference; 10-15 September 2006; Manchester. pp. 1410-1413
- [3] Loecker C, Knott P, Sekora R, Algermissen S. Antenna design for a conformal antenna array demonstrator. In: 6th European Conference on Antennas and Propagation (EuCAP); 26-30 March 2012; Prague. pp. 151-153
- [4] Salonen P, Rahmat-Samii Y, Schaffrath M, Kivikoski M. Effect of textile materials on wearable antenna performance: A case study of GPS antennas. In: IEEE International Symposium on Antennas and Propagation; 20-25 June 2004; Monterey. pp. 459-462
- [5] Kennedy TF, Fink PW, Chu AW, Champagne NJ, Lin GY, Khayat MA. Body-worn E-textile antennas: The good, the low-mass, the conformal. *IEEE Transactions on Antennas and Propagation*. 2009;57:910-918. DOI: 10.1109/TAP.2009.2014602
- [6] Psychoudakis D, Lee GY, Chen C-C, Volakis JL. Estimating diversity for body-worn antennas. In: 3rd European Conference on Antennas and Propagation (EuCAP); 23-27 March 2009; Berlin. pp. 704-708
- [7] Semkin V et al. Conformal antenna array for millimeter-wave communications: Performance evaluation. *International Journal of Microwave and Wireless Technologies*. 2017;9:241-247. DOI: 10.1017/S1759078715001282
- [8] Kuang Y, Yao L, Yu SH, Tan S, Fan XJ, Qiu YP. Design and electromagnetic properties of a conformal ultra wideband antenna integrated in three-dimensional woven fabrics. *Polymers*. 2018;10:1-10. DOI: 10.3390/polym10080861
- [9] Schippers H, Verpoorte J, Jorna P, et al. Conformal phased array with beam forming for airborne satellite communication. In: International ITG Workshop on Smart Antennas (WSA 2008); 26-27 February 2008; Vienna. pp. 343-350
- [10] Salas Natera MA et al. New antenna array architectures for satellite communications. In: Karimi M, editor. *Advances in Satellite Communications*. 1st ed. London, UK: IntechOpen; 2011. pp. 167-194. DOI: 10.5772/838
- [11] Wu Y, Warnick F, Jin C. Design study of an L-band phased array feed for wide-field surveys and vibration compensation on FAST. *IEEE Transactions on Antennas and Propagation*. 2013;61:3026-3033. DOI: 10.1109/TAP.2013.2254438
- [12] Braaten BD, Aziz MA, Roy S, Nariyal S, Irfanullah, Chamberlain NF, et al. A self-adapting flexible (SELFLEX) antenna array for changing conformal surface applications. *IEEE Transactions on Antennas and Propagation*. 2013;61:655-665. DOI: 10.1109/TAP.2012.2226227
- [13] Anagnostou D, Iskander M. Adaptive flexible antenna array system for deformable wing surfaces. In: IEEE Aerospace Conference; 7-14 March 2015; Big Sky, MT. pp. 1-6
- [14] Irfanullah, Khattak S, Braaten BD. Improvement of the broadside radiation

pattern of a conformal antenna array using amplitude tapering. *Applied Computational Electromagnetics Society Journal*. 2017;**32**:511-516

[15] Braaten BD, Roy S, Irfanullah, Nariyal S, Anagnostou DE. An autonomous self-adapting conformal array for cylindrical surfaces with a changing radius. In: *IEEE Antennas and Propagation Society International Symposium (APSURSI)*; 6-11 July 2014; Memphis. pp. 1784-1785

[16] Braaten BD, Roy S, Irfanullah, Nariyal S, Anagnostou DE. Phase compensated conformal antennas for changing spherical surfaces. *IEEE Transactions on Antennas and Propagation*. 2014;**62**:1880-1887. DOI: 10.1109/TAP.2014.2298881

[17] Josefsson L, Persson P. *Conformal Array Antenna Theory and Design*. 1st ed. Hoboken, New Jersey, United States: Wiley-IEEE Press; 2006. 472 p. DOI: 10.1002/047178012X

[18] Haupt RL. *Antenna Arrays, A Computational Approach*. 1st ed. Hoboken, New Jersey, United States: Wiley-IEEE Press; 2010. 534 p. DOI: 10.1002/9780470937464

[19] Seidel TJ, Rowe WST, Ghorbani K. Passive compensation of beam shift in a bending array. *Progress in Electromagnetics Research C*. 2012;**29**:41-53

[20] Ferreira DB, de Paula CB, Nascimento DC. Design techniques for conformal microstrip antennas and their arrays. In: Kishk A, editor. *Advancement in Microstrip Antennas with Recent Applications*. 1st ed. London, UK: IntechOpen; 2013. pp. 1-31. DOI: 10.5772/53019

[21] Khaleel HR, Al-Rizzo HM, Abbosh AI. Design, fabrication, and testing of flexible antennas. In: Kishk A, editor. *Advancement in Microstrip*

Antennas with Recent Applications. 1st ed. London, UK: IntechOpen; 2013. pp. 363-382. DOI: 10.5772/50841

[22] Irfanullah, Nariyal S, Roy S, Masud MM, Ijaz B, Iftikhar A, et al. A note on the fundamental maximum gain limit of the projection method for conformal phased array antennas. In: *Proceedings of the IEEE International Conference on Wireless Information Technology and Systems (ICWITS)*; 11-16 November 2012; Maui, HI. pp. 1-4

[23] Rigobello F, Mansutti G, Khan MS, Capobianco AD. Pattern recovering of conformal antenna array for strongly deformed surfaces. In: *11th European Conference on Antennas and Propagation (EuCAP)*; 19-24 March 2017; Paris. pp. 869-871

[24] Mansutti G, Rigobello F, Asif S, Khan MS, Capobianco AD, Galtarossa A. Main lobe control of a beam tilting antenna array laid on a deformable surface. *International Journal of Antennas and Propagation*. 2018;1-6. DOI: 10.1155/2018/2521953

[25] Mansutti G, Khan MS, Capobianco AD, Iftikhar A, Asif S. Self-adapting conformal phased array antennas for complex changing surfaces. *Microwave and Optical Technology Letters*. 2017;**59**:393-399. DOI: 10.1002/mop.30301

[26] Chiba I, Hariu K, Sato S, Mano S. A projection method providing low sidelobe pattern in conformal array antennas. In: *International Symposium Digest: Antennas and Propagation*; 26-30 June 1989; San Jose. pp. 130-134

[27] Liang Z, Ouyang J, Yang F. A hybrid GA-PSO optimization algorithm for conformal antenna array pattern synthesis. *Journal of Electromagnetic Waves and Applications*. 2018;**32**:1601-1615. DOI: 10.1080/09205071.2018.1462257

[28] Xu Z, Li H, Liu Q-Z. Pattern synthesis of conformal antenna array by the hybrid genetic algorithm. *Progress in Electromagnetics Research (PIER)*. 2008;79:75-90. DOI: 10.2528/PIER07091901

[29] Mandrić V, Rupčić S, Žagar D. Optimization of the spherical antenna arrays. In: *Proceedings of 54th International Symposium ELMAR-2012*; 12-14 September 2012; Zadar. pp. 287-292

[30] Haupt RL. Adaptive antenna arrays using a genetic algorithm. In: *IEEE Mountain Workshop on Adaptive and Learning Systems*; 24-26 July 2006; Logan, UT

[31] Hansen RC. *Phased Array Antennas*. 1st ed. Logan, UT, USA: John Wiley & Sons, Inc.; 2009. 551. p. DOI: 10.1002/9780470529188

[32] Boyd S, Vandenberghe L. *Convex Optimization*. 1st ed. New York: Cambridge University Press; 2004. 716 p. DOI: 10.1017/CBO9780511804441